Chapter-3

Experimental Setup & Methodology

3.1 Introduction

This chapter describes the experimental details related to the present investigation, including lead-free solder preparation, electrochemical and non-electrochemical, and also various characterization optical microscopes, Scanning Electron Microscopy (SEM) with Energy Dispersive X-ray spectroscopy (EDX), X-ray diffraction (XRD), X-ray photoelectron spectroscopy (XPS), potentiodynamic polarization, immersion test, and electrochemical impedance spectroscopy (EIS) analysis are described.

3.2 Preparation of lead-free solder alloys

3.2.1 Raw materials selection

All raw materials for the preparation of lead-free solder alloys were obtained from initial purity and suppliers shown in table 3.1.

Table3.1 Purity and Supplier of the solder alloys

S.No	Materials	Initial purity (%)	Supplier	Physical State
1	Sn	≥ 99.99	Alfa Aesar, UK	Shot
2	Cu	≥ 99.99	Alfa Aesar, UK	Shot
3	In	≥ 99.99	Johnson Matthey, UK	Ingots
4	Al	≥ 99.99	Alfa Aesar, UK	Shot
5	Zn	≥ 99.98	Alfa Aesar, UK	Shot
6	NaCl	≥ 99.99	Molychem, India	Powder
7	KCl	≥ 99.99	Molychem, India	Powder

3.2.2 Synthesis of Lead-free Solder alloys

The solder metals are weighed individually according to their weight fraction in alloys. For simplicity, the whole sample can be divided into three ternary alloys. Each ternary alloy consists of four samples. First ternary alloys contain Sn-0.7Cu-xIn, In weight percentage is varied as 0.0, 1.0, 2.0 and 3.0. In the same way, weight percent variation of Al and Cu have been done in second Sn-0.7Cu-xAl and third Sn-9Zn-xCu ternary alloys, respectively as shown in Fig 3.1.

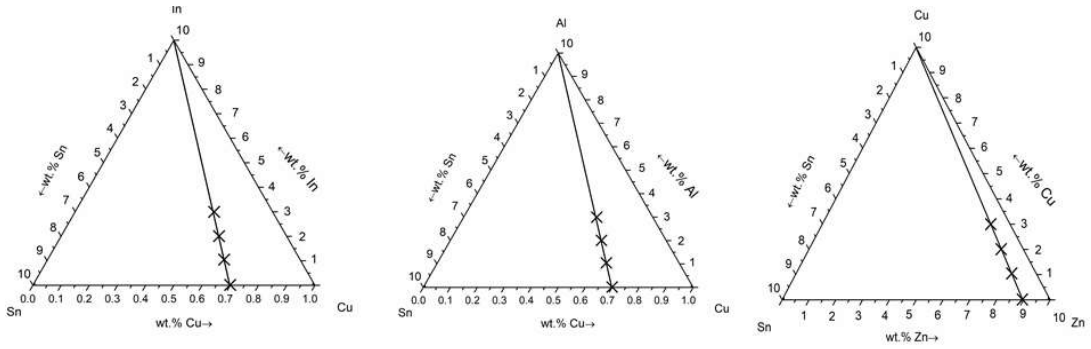

Fig.3. 1 (a) Sn-0.7Cu-xIn (b) Sn-0.7Cu-xAl (c) Sn-9Zn-xCu solder alloys.

3.2.3 Melting of Lead-free solder alloys

All lead-free solder alloys were prepared using a vacuum induction melting furnace of pure Sn, Cu, In, Al and Zn according to the composition of solder alloys. All virgin raw materials were weighed with an accuracy of ± 0.0001g, kept in an alumina crucible (5 cm height and 2 cm diameter), and then put in a furnace chamber.

A Vacuum level of 10^{-4} torr was maintained inside the furnace, followed by nitrogen gas purging to remove oxygen and unwanted gases to prevent oxidation of solder alloys in the furnace chamber. The temperature of the furnace was maintained at 800^0C for the melting of alloys. A heating rate of 5^0C/min was followed during the heating of the furnace. A socking time of 30 min was allowed at 800^0C for all alloys. The furnace was then allowed to cool down to 250^0C. After that, samples were furnace cooled. All the processes for melting the alloys were repeated three times under the same condition to achieve sample homogeneity. The alumina crucible was broken to remove the solidified solder alloys. Solder alloys were subsequently cleaned, ground, and polished for further analysis and characterization.

3.3 Microstructure Characterization

3.3.1 Optical Microstructure

Prepared samples were cut in 2cm diameter, and 0.1 cm thickness and cold mounted using epoxy resin. The working surface area was mechanically (belt) grinding with sandpaper to remove unwanted material; after that, 400-2500 grid SiC paper with 0.3µm Al_2O_3 was used for archived mirror-like surface and etched with 2%HCl + 5% HNO_3 + 95% C_2H_5OH solution for 2-3 sec for microstructure analysis using an optical microscope (OM, Leica Z6 APO) shown in Fig. 3.2. The Leica Z6 APO is an apochromatic zoom system with superb light transmission for high contrast, high resolution, and deep analysis. The single beam path produces 2D images and eliminates parallax. This is ideal for digital imaging combined with the Leica DFC cameras and the Leica Applications Suite. The modular architecture allows for a custom configuration for each application. The highest brightness levels are achieved when a digital camera is directly attached. The attachment of a binocular tube from the Stereomicroscope line is used for visual examination duties.

Fig.3. 2 Optical Microscope (OM, Leica Z6 APO)

3.3.2 Scanning Electron Microscope (SEM)

The scanning electron microscope (SEM) is an electron microscope that uses a high-energy electron beam to examine a specimen shown in Fig. 3.3. It is used to create a two-dimensional image of any size and thickness of the example. The electrons propelled by

electric and magnetic fields interact with the sample, producing signals that carry information on the surface or near-surface topography, composition, and other qualities such as electrical conductivity. The structure of bulk specimens is typically studied using SEM. It can produce pictures of the sample surface with less than 1nm resolution and provide information on particles as small as 1nm. A standard SEM with a magnification range of 10x – 200,000x and a spatial resolution of 50 – 100 nm can scan areas ranging in width from 1cm to 5m. Secondary electrons, backscattered electrons, specific X-rays, and light are some indications produced by an SEM (cathode luminescence). Secondary electron imaging is the mode utilized in SEM micrographs.

Before and after corrosion tests, the lead-solder alloy samples were mechanically polished using standard metallographic techniques. The sample micrographs were obtained. Secondary electron imaging is the mode performed in SEM micrographs.

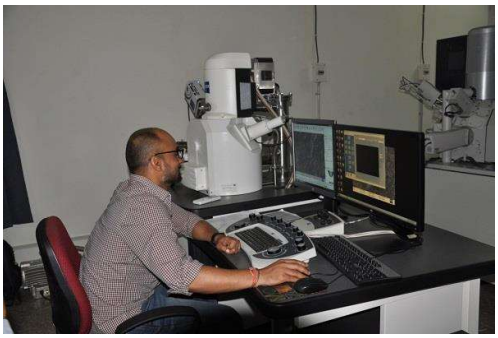

Fig.3. 3 Scanning Electron Microscope (SEM, ZEISS MA15/18, UK)

3.4 Corrosion behaviour

3.4.1 Non-Electrochemical Method

Non-electrochemically (static Immersion) samples were exposed to a corrosive medium, and the corrosion rate was determined by the conventional weight loss/gain method. This technique calculates the difference between the sample's initial and final weight due to exposure to a known surface area in a corrosive environment for a certain period.

Corrosion rate, or the rate at which material is removed due to chemical action, is a crucial corrosion characteristic. The corrosion penetration rate (CPR), or the thickness loss of material per unit of time, can represent this.

This calculation's formula is as follows:

$$\mathrm{CPR} = \frac{\mathrm{KW}}{\rho \mathrm{At}} \tag{3.1}$$

Where

- K = Corrosion Constant
- W = Weight difference between before and after exposure of samples
- ρ = Density of samples
- A = Exposes samples area
- t = exposes times of samples

Fig.3. 4 Immersion Test equipment

Table3.2 Corrosion penetration rate parameters unit.

K Value	Units				
	W	ρ	A	t	CPR
534	mg	g/cm^3	in^2	h	Mils per year (mpy)
87.6	mg	g/cm^3	cm^2	h	Millimeters per year (mm/y)

3.4.2 Electrochemical corrosion behaviour

According to electrochemical corrosion, corrosion occurs due to electrochemical processes, including an anodic or oxidation reaction and a cathodic or reduction reaction, which are described as a given metal M in a NaCl solution.

$M \rightarrow M^{+} + e^{-}$ Anodic Reaction (Oxidation) (3.2)

$2H^{+} + 2e^{-} \rightarrow H_2$ cathodic reaction (Reduction) (3.3)

Eq. (3.2) and (3.3) are partial reactions that must occur on the metal surface simultaneously and at the same rate; otherwise, the metal will become charged, which is impossible. This brings us to the most fundamental concept of corrosion. "During corrosion, the rate of oxidation matches the rate of reduction"; hence an electrochemical reaction may be separated into two or more partial oxidation and reduction processes. More than one oxidation and reduction may occur during corrosion. Because these processes are mutually dependent, lowering the rates of either of them can help to minimize corrosion. Wagner and Traud created the well-known 'Mixed potential theory' for interpreting corrosion processes by superimposing partial electrochemical methods. This theory assumes that any electrochemical process may be split into two or more partial oxidation and reduction steps. There is no net accumulation of electric charge during the electrochemical process.

The following are the most regularly used electrochemical methods for determining corrosion rates.

1. Potentiodynamic polarization
2. Electrochemical Impedance Spectroscopy

3.4.2.1 Potentiodynamic Polarization

During electrochemical corrosion, the anode and cathode at the metal's surface are not at their equilibrium potential. Polarisation is the term for this divergence from the equilibrium potential. Polarisation is defined as the amount of potential difference or electrode potential displacement induced by net current flow to or from an electrode measured in volts, also known as overvoltage or overpotential and expressed by η. Polarisation is a critical corrosion metric that allows researchers to understand the corrosion rate better.

Polarization can be divided into three categories:

1. **Activation polarization**

This is an electrochemical process in which the sequence of reactions at the metal-electrolyte contact controls the outcome. In other words, a delayed electrode reaction induces activation polarization because the electrode reaction requires activation energy. Activation polarization can affect both anodic and cathodic processes.

2. **Concentration Polaraization**

This is noticed when electrochemical processes are regulated by diffusion in the electrolyte. This behavior is standard when the concentration of reducible species in the environment is low, such as in aerated salt solutions.

3. **Resistance Polarization**

An ohmic potential drop usually occurs through a portion of the electrolyte surrounding the electrode, a metal reaction product coating on the surface, or both polarization of resistance

$$\eta_R = RI = \gamma i \qquad (3.4)$$

Where

- η_R = Resistance Polarization
- R = film resistance for electrode surface in ohms
- I = current in Amperes
- Γ = Film resistance in ohm/ cm^2

There are two methods used to measure corrosion rate.

- Tafel extrapolation
- Linear Polarization

3.4.2.1.1 Tafel Extrapolation

Wagner and Traud utilized this method to test the Mixed Potential Theory. To create a Tafel plot for a metal specimen, polarize the sample to roughly 300 mV anodically and cathodically from the corrosion potential E_{corr}, as illustrated in Fig. 3.5. The corrosion current density i_{corr} can be calculated by extrapolating the Tafel region in either a cathodic or anodic polarization curve to the corrosion potential.

The Tafel equations describe the anodic and cathodic Tafel graphs.

$$\eta = \beta \log(i/i_{corr}) \quad (3.5)$$

$$\eta = \beta\ (\log i - i_{corr}) \quad (3.6)$$

Where

η = over-voltage, the difference between the specimen's potential and the corrosion potential

β = Tafel Constant

i = current density at over voltage in $\mu A/cm^2$ or rate of oxidation or reduction in terms of current density at η.

i_{corr} = Corrosion current density in $\mu A/cm^2$

When $\eta = 0 \ (E_{corr})$ (3.7)

Then $0 = \log (i/i_{corr})$ (3.8)

$i = i_{corr}$ (3.9)

For both the anodic and cathodic regions of the Tafel plot, Tafel Constants, denoted by β_a and β_c, respectively, can be determined. The Tafel constant is measured in mV/decade or V/decade.

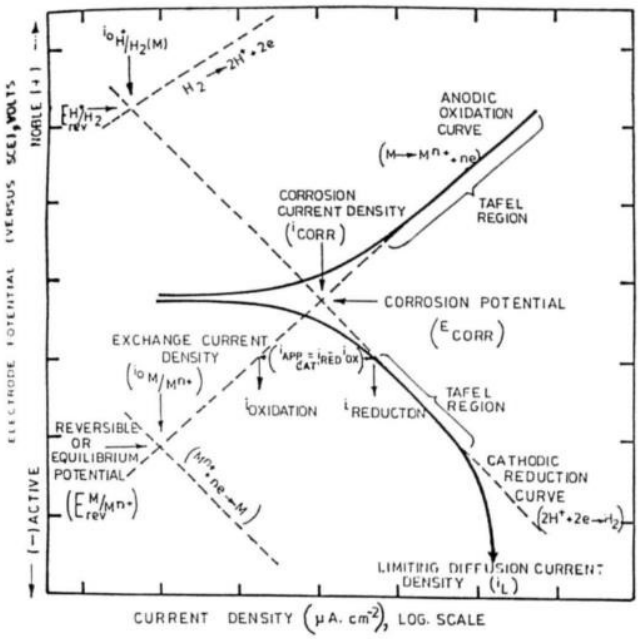

Fig.3. 5 Polarization curve with different technology

The following are some of the drawbacks of Tafel plots:

- Polarisation of the test specimen by several hundred mV from the corrosion potential can cause enough disturbances in the system to distort subsequent periodic measurements done with the same specimen.
- The combination of concentration polarisation and IR falls can restrict the linear region to the point where extrapolation to i_{corr} is problematic.

- Extrapolation of the anodic and cathodic linear Tafel regions may not meet at E_{corr} sometimes.
- Obtaining data for each polarisation curve takes several hours, although faster than weight loss methods. In many circumstances, especially in-plant applications, this may not be practical.

3.4.2.1.1 Linear Polarization

The linear polarisation approach, also known as the polarisation resistance method, can largely overcome the drawbacks of the Tafel extrapolation method. This approach was created in the mid-1960^{s} and has since evolved significantly. The principle behind this method is that the applied current is a linear function of the electrode potential within 10 mV, more noble or active than the corrosion potential. Fig. 3.6 depicts this. The corrosion potential is utilized as an over-voltage reference point in this diagram. A plot of overvoltage vs. applied anodic and cathodic current (i_{appl}) on a linear scale is displayed. The initial 20 mV polarisation of the curve depicted in Fig. 3.5 is represented in this graphic. Stern and Geary derived the following equation from connecting the slope of the linear polarisation curve to the system's kinetic characteristics.

$$\frac{\Delta E}{\Delta i_{appl}} = \frac{1}{2.302 i_{corr}} \frac{\beta_a \beta_b}{\beta_a + \beta_b} \tag{3.10}$$

Where Δi_{appl} is the observed external current flowing due to this potential shift, and ΔE is the potential shift from the corrosion potential E_{corr}. The Tafel slopes of the anodic and cathodic reactions are βa and βc, respectively.

$\frac{\Delta E}{\Delta i_{appl}}$ Is the slope of the linear polarization plot, and icorr is the corrosion current density.

If I value is known, corrosion current density can be calculated using the form equation.

The slope of the linear polarization curve $\frac{\Delta E}{\Delta i_{appl}}$ is mainly controlled by icorr and relatively insensitive to changes in β values.

$$\frac{\Delta E}{\Delta i_{appl}} = \frac{0.0126}{i_{corr}} \tag{3.11}$$

Without knowing the electrode kinetic parameters, Eq (3.11) may be used to calculate the corrosion resistance. Though the method's precision may be insufficient, Eq (3.11) gives a unique basis for determining relative corrosion rates efficiently.

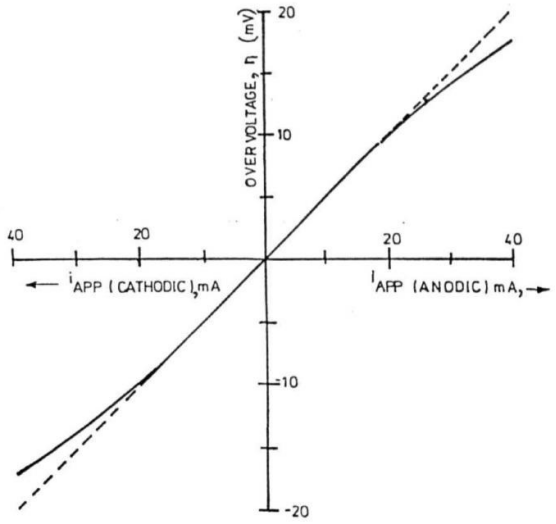

Fig.3. 6 Linear polarization diagram

3.4.2.2 AC Impedance Spectroscopy method

The polarisation resistance approach frequently produces incorrect findings for highly high electrolyte resistance systems. In these circumstances, ac impedance measurements are helpful. When applied to the study of electrochemical methods, they may yield a wealth of kinetic and mechanistic information. As a result, the approach is rapidly gaining popularity in corrosion research.

Compared to dc approaches, the ac impedance approach has a few unique advantages:

1. The ac impedance approach employs very low excitation amplitudes, often in the 5 to 10 mV peak to peak range. The electrochemical test system is only a little perturbed by excitation amplitudes of this scale, decreasing measuring technique-related errors.
2. Ac impedance tests give essential mechanistic information by providing data on both electrode capacitance and charge transfer kinetics.
3. Because the approach does not require a potential scan, measurements in low conductivity solutions where dc methods are prone to substantial potential-control mistakes can be made. In reality, the ac impedance approach may be used to estimate an electrochemical cell's uncompensated resistance.

The analogous electrical circuits of electrochemical systems can be investigated. The circuit depicted in Fig. 3.6 might be used to represent a rudimentary system. Between the working electrode and the reference electrode, R_1 is the uncompensated resistance. At the electrode/solution contact, R_Ω is the polarization resistance. The double-layer capacitance at this interface might be represented as C_{dl}. Knowing R_p allows you to calculate electrochemical reaction rates. Capacitance measurements can reveal information about the mechanisms that lead to film formation at the electrode.

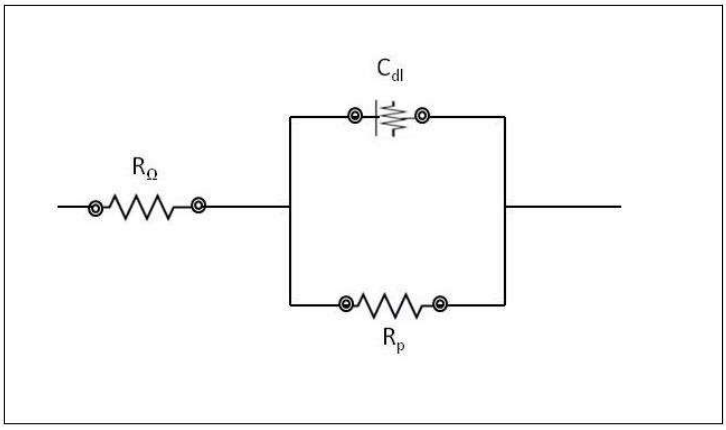

Fig.3. 7 Equivalent electronic circuit for a simple electrochemical cell

An ac impedance experiment may be used to identify the values of various elements in an equivalent circuit or to simply test that a given electrochemical system matches a specific equivalent-circuit model. This is accomplished experimentally by examining the electrochemical system's response to ac excitation across a wide frequency range. An ac voltage or an ac current can be used to excite the system. The measured response will be an ac current or an ac voltage, which may be used to compute the system impedance. Both in-phase and quadrature impedance components at various frequencies across the necessary range are required for a complete description of the electrochemical system's behaviour. The following equation may be used to compute them from the real and imaginary components of the excitation and response waveforms.

$$Z_{total} = Z' + Z'' \quad (3.12)$$

where Z_{total} is the total ac impedance vector, Z' and Z" are the real and imaginary components of the impedance vector, and Z_{total} is the total ac impedance vector Impedance data in the range of 0.001 to 10^4 Hz may be used to describe most electrochemical systems.

The impedance data can be plotted in several forms. Each format has its own set of benefits for disclosing the unique properties of a test system. Fig. 3.8 depicts an ac impedance profile for a basic electrochemical system in Nyquist form, while Fig. 3.9 depicts it as a Bode plot, as detailed below.

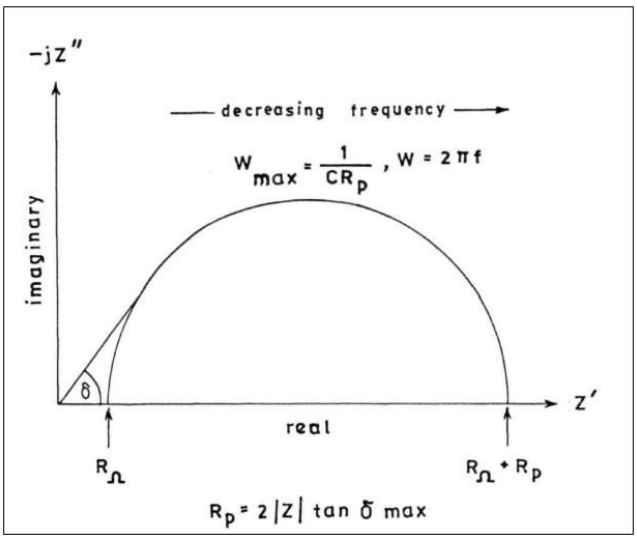

Fig.3. 8 Impedance profile for a simple electrochemical system in the form of Nyquist plot.

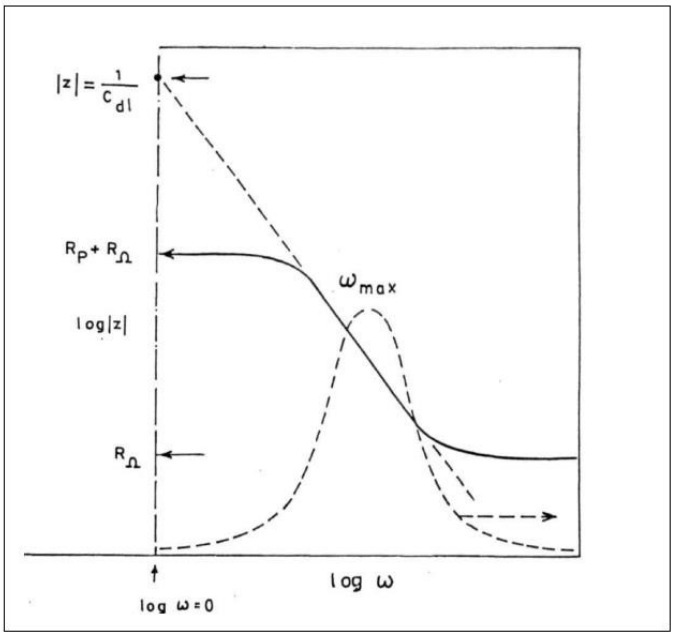

Fig.3. 9 Impedance profile for a simple electrochemical system in the form of Bode plot.

3.4.2.2.1 The Nyquist Plot

A Cole-Cole plot or a complex impedance plane diagram is another name for this type of graphic. At each excitation frequency, the imaginary component of impedance (Z") is

shown against the real component of impedance (Z'). The uncompensated resistance between the working electrode and the reference electrode, R_Ω, the polarisation resistance at the electrode/solution interface, Rp, and the double layer capacitance at this interface, C_{dl} may all be calculated using this Fig. 3.8 Knowing Rp allows you to calculate electrochemical corrosion reaction rates.

It is obvious from Fig. 3.9 that only uncompensated resistance contributes to the actual component of impedance at high frequencies, whereas polarization resistance contributes to this measurement at extremely low frequencies. The polarization resistance (R_p) becomes visible to the method when the excitation waveform is substantially quicker than the charge-transfer rate. On the other hand, an ohmic resistance (R_Ω) represents constant impedance at all frequencies. This is in line with the fact that R_P can be measured using the dc method, but R_Ω cannot.

3.4.2.2.2 The Bode plot

The Bode plot, which is a plot of log $|Z|$ Versus log w is a handy alternative to the Nyquist plot for avoiding lengthier measurement durations associated with low-frequency Rp calculations. It enables more accurate data extrapolation from higher frequencies. This plot type allows you to look at the absolute impedance $|Z|$ And the phase shifts as determined by the equation below.

$$|Z| = \sqrt{(Z')^2 + (Z'')^2} \text{ And } \tan\theta = \frac{Z''}{Z'} \qquad (3.12)$$

Each as a function of the frequency of the resulting waveform Rp and Ru may be calculated using the log $|Z|$ vs. logw curve. The "break-point" of this curve at intermediate frequencies should be a straight line with a slope. The value of C_{dl} is

obtained by extrapolating this line to the log $|Z|$ axis at w= 1 (log w=0) from the relationship.

$$Z = \frac{1}{Cdl} \tag{3.13}$$

3.5 Surface Characterization

3.5.1 X-Ray Diffraction (XRD)

XRD is an essential tool for determining phase analysis (elemental phase/ intermetallic phase/ crystalline phase/ non-crystalline phase), lattice parameter determination, strain determination, texture and orientation estimation, and order-disorder transition in materials. The solder alloys were characterized using a Phillips Pan analytical PW3040/00 X-ray diffractometer shown in Fig. 3.10. In x-ray diffraction, copper filtered Cu-Kα radiation was used. We used a scanning range of 2θ from 20 to 90 degrees with a scanning speed of 5 degrees per minute and a 40 kV accelerating voltage and 15Amps Current during the XRD examination. The peak was analyzed using X-pert high score software to detect distinct phases

Fig.3. 10 Benchtop X-ray diffraction (BT-XRD)

3.5.2 X-Ray Photoelectron Spectroscopy (XPS)

The X-ray photoelectron spectroscopy (XPS) technique, also known as electron spectroscopy for chemical analysis (ESCA), examines a material's surface chemistry. As shown in Fig. 3.11, XPS can determine a material's elemental composition and its atoms'

chemical and electronic states. By irradiating a solid surface with an X-ray beam and detecting the kinetic energy of electrons released from the top 1-10 nm of the material, XPS spectra can be obtained. Counting expelled electrons over a range of kinetic energies produces a photoelectron spectrum. The photoelectron peaks' energies and intensities allow identifying and quantifying all surface elements (except hydrogen).

Fig.3. 11 X-ray photoelectron spectroscopy (XPS, Thermo Fisher Scientific)